JOURNAL OF MATERIALS SCIENCE 29 (1994) 1115–1120

The dependence of the strength of zinc sulphide on temperature and environment

C. S. J. PICKLES, J. E. FIELD
Cavendish Laboratory, University of Cambridge, Madingley Road, Cambridge CB3 OHE, UK

The dependence of the strength of zinc sulphide on temperature, environment, surface finish and specimen size has been assessed. Room-temperature fracture stresses were determined using a bursting disc geometry for a number of different surface finishes and for two different sample sizes. High- and low-temperature fracture stresses in a dry nitrogen atmosphere were obtained from experiments using the Brazilian test geometry and showed that the average strength of the material remained above or equal to the room-temperature value within the range −70 to +600 °C. The Brazilian test is an indirect tensile technique which is attractive for its experimental simplicity but gives fracture stress values which are consistently below those obtained by direct tensile techniques. The data from this test were therefore compared at room temperature to results obtained from the bursting disc test on samples which had been prepared using the same techniques. The possibility of delayed failure through environmentally enhanced slow crack growth was evaluated using the double-torsion technique which revealed slow crack growth below the critical stress intensity factor.

1. Introduction

Zinc sulphide is used extensively in aerospace applications. Its optical and thermal properties are ideally suited for its role as an infrared window material, but it is both weak and soft and is therefore susceptible to the numerous static and impact stresses imposed on the component by high-velocity flight.

The surface of an aircraft can experience both low and high temperatures and environments of different humidities. The experiments described below investigate the variation of the strength of the material with a number of relevant parameters.

The measured strength of a material is governed by its critical stress intensity factor and the flaw distribution in a particular sample. This distribution can vary greatly between specimens prepared by different grinding and polishing procedures especially for specimens of different dimensions. A biaxial tensile test was therefore used to evaluate the strength of test specimens from a range of sources as well as full-size components.

Slow crack growth can occur in some materials at stress intensity factors below the critical value (see, for example, [1–5]) in certain environments and the extent of this "stress corrosion" effect in zinc sulphide was evaluated using the double-torsion test.

In addition, the variation of zinc sulphide tensile strength with temperature was investigated using the Brazilian test, an indirect tensile geometry which has simple gripping arrangements, allows the use of small samples and hence increases the number of samples available for test. This gave sufficient data points at each temperature to enable small changes in strength to be detected despite the spread in strength typical of brittle materials.

In earlier work from this laboratory, van der Zwaag *et al.* [6] described indentation contact damage in zinc sulphide, van der Zwaag and Field [7] the liquid impact damage in zinc sulphide, and Townsend and Field [8] the fracture toughness and hardness of zinc sulphide as a function of grain size. A summary of rain erosion damage mechanisms in brittle materials and of recent high-velocity rain drop impact on zinc sulphide can be found elsewhere ([9, 10] references therein).

2. Experimental procedure

2.1 Fracture stress assessment (room temperature)

Room-temperature fracture stress measurements were performed using the bursting disc test shown schematically in Fig. 1 [11]. In this test, a disc is supported around its circumference and the reverse side is pressurized by a hydraulic fluid behind a neoprene diaphragm. The resultant stress distribution on the circumferentially supported side is tensile over most of the disc. This technique, therefore, has the advantage that it samples flaws over a large area of the disc. Because failure does not necessarily occur in the centre of the disc, the position and orientation of the flaw at which fracture initiated must be identified to allow the stress at that point at the moment of failure to be calculated. In our work this is routinely performed by a computer programme following measurement of the

0022–2461

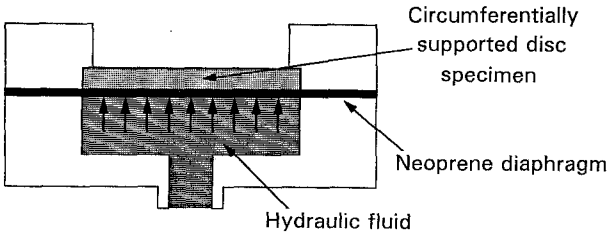

Figure 1 The bursting disc geometry.

specimen dimensions and the flaw position and orientation.

2.2. Evaluation of stress corrosion

The double-torsion technique [12, 13] was selected to evaluate the stress corrosion characteristics of zinc sulphide. This geometry is shown in Fig. 2 and is particularly useful for slow crack growth studies because for a significant portion of the crack path, the stress intensity factor is independent of the crack length. Both constant load and load-relaxation applications were used to extract crack velocity against stress intensity factor data. Load relaxation provides several data points per specimen but can only be used at moderately high crack velocities and at low velocities the constant-load technique must be used. The crack front is curved and the velocity is therefore not constant through the thickness of the plate as is assumed by theory. In this case, the crack velocity was taken as that at the tensile face of the slab as recommended by Tait *et al.* [14] and Michalske *et al.* [15].

The double-torsion technique is often used with grooves on one or both faces of the sample to force the crack to propagate down the centre of the plate. Fuller [12] suggested that these grooves could influence the crack growth by introducing stress concentrations into the sample and that it would be preferable to rely on accurate alignment of the loading points to ensure the required crack path. This was facilitated in the present experiments by using a specimen preparation procedure described by Quinn [16]. In this the sample is carefully notched to a depth of 5 mm and a Knoop indentor under a 1 kg load is pulled across the specimen to create a 5 mm scratch leading from the end of the notch (see Fig. 2). The specimen is then slowly loaded in the double-torsion rig until a pre-crack forms following the scratch rather than the randomly oriented machining cracks at the end of the notch. The alignment of the notch, the scratch, the pre-crack and the loading points must be extremely accurate for the experiment to be successful.

For results from the double-torsion technique to be valid, due consideration must be given to selection of specimens of the optimum dimensions, correcting for the thickness of the specimen, and the portion of the crack length over which the stress intensity factor is constant. The present study follows the guidelines given in the literature review by Tait *et al.* [14].

2.3. Fracture stress assessment (high temperature)

The hydraulic nature of the bursting disc apparatus makes it unsuitable for fracture stress measurements at elevated temperatures. The Brazilian test geometry (Fig. 3 [17, 18]), implemented on an Instron universal testing machine, was therefore selected for this second experiment. In this geometry, a small disc (15 mm diameter and 3 mm thick in the present experiments) was compressed between curved anvils [19] causing tensions perpendicular to, and failure along the loading axis. The results obtained from indirect tensile tests such as this are often unreliable as absolute measures of fracture stress [20], but the geometry is valid for assessing the *variation* in strength of a single material with temperature as in the present study. It is, however, important to ensure that the specimen fails at the centre of the disc in a tensile manner, rather than through crushing at the anvils. This crushing could be avoided by using curved rather than flat anvils [19] and inserting padding between the anvil and the specimen [21]; in this case, asbestos paper was used. Because the Brazilian test results are often low compared

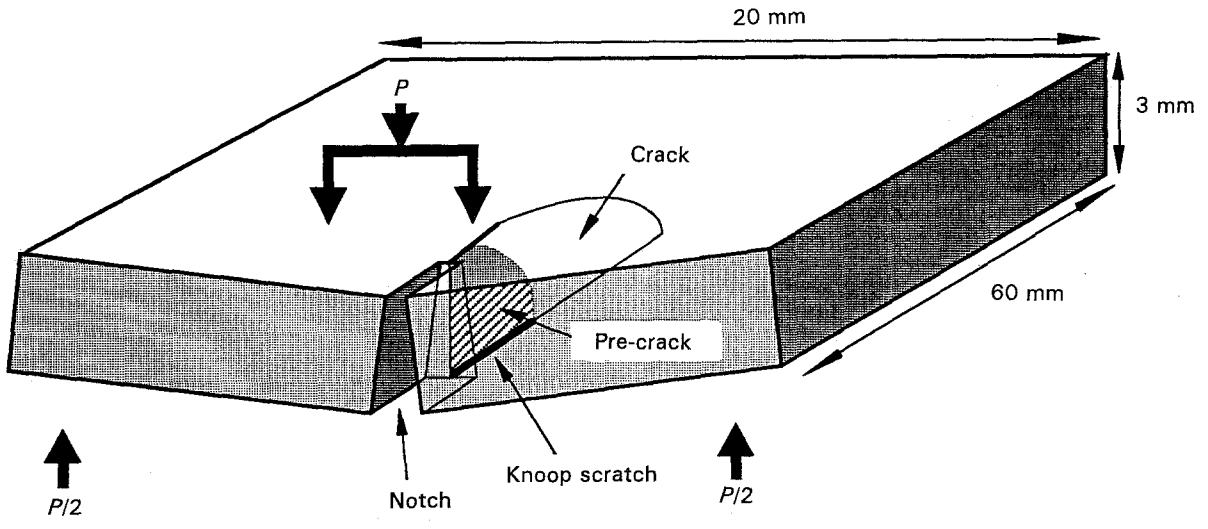

Figure 2 The double-torsion geometry showing specimen dimensions.

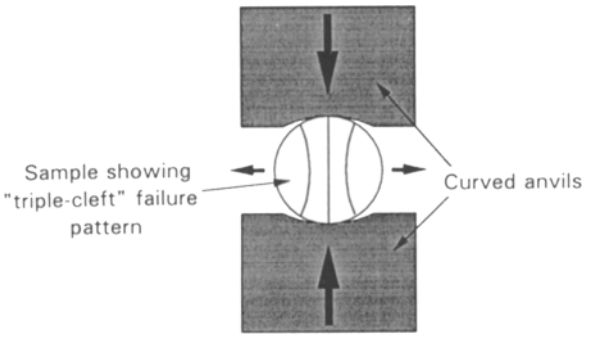

Figure 3 The Brazilian test geometry.

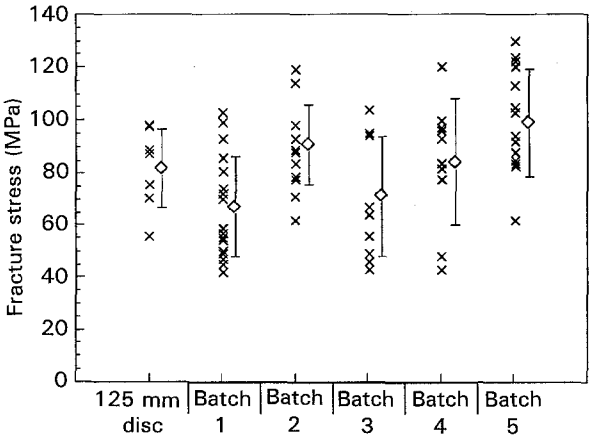

Figure 4 The variation in fracture stress of different batches of zinc sulphide.

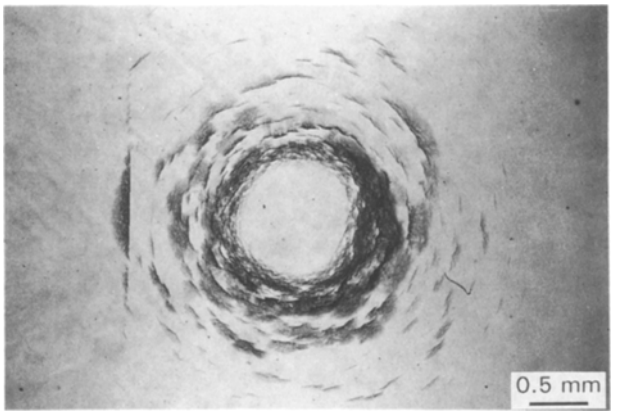

Figure 5 A typical damage site on zinc sulphide caused by the impact a 310 m s^{-1} liquid jet from a 0.8 mm nozzle. Note the long linear crack caused by the poor surface finish.

to other techniques for measuring fracture stress, a baseline result was obtained from samples of the same batch of material with the same surface finish tested in the bursting disc apparatus. Earlier experiments in the laboratory by Hand [22] on glasses, zinc sulphide and germanium, showed that the Brazilian test produces strength results approximately 65% of those from the bursting disc apparatus.

Elevated temperatures were simply obtained by enclosing the anvils in an oven controlled by both free-standing and anvil-mounted thermocouples and calibrating the temperature gradient with a dummy instrumented sample. Low temperatures were obtained by wrapping cooling coils around the anvils through which liquid nitrogen was passed, the flow being controlled by the same thermocouple arrangement used above in conjunction with a cryogenic solenoid.

Zinc sulphide is susceptible to rapid oxidation at elevated temperatures and for these experiments it was required that this factor be removed. The experiments were therefore performed in an enclosed chamber which after repeated evacuation and flushing with oxygen-free dry nitrogen was left at positive pressure during the heating and loading phase. The relative humidity within the chamber was reduced to $\sim 5\%$ at room temperature by this process. The loading of the samples to failure took typically 60 s.

3. Results

3.1. The variation in strength of zinc sulphide samples

Samples from five batches of zinc sulphide, finished using different techniques by different manufacturers, were broken in the bursting disc apparatus. The samples were in the form of discs 25 mm diameter by 2 mm thick.

Batch 1 Barr and Stroud, Glasgow.
Batch 2 British Aerospace, Stevenage.
Batch 3 Barr and Stroud finished by Vintens.
Batch 4 Barr and Stroud finished to Royal Signal and Radar Establishment, Malvern Specifications.
Batch 5 British Aerospace material with diamond-fly cut finish.

Fig. 4 contains the average fracture stress and standard deviation for batches 1–5 as well as the individual data points. It can immediately be seen that there is a large spread in the results and some of the discs fail at quite low fracture stresses. Batch 1 had the same surface preparation as the discs used in the Brazilian test in Section 3.3 and the fracture stress of 67 ± 19 MPa (where the error is the standard deviation of the data) is therefore the baseline for that experiment.

The reasons for this low strength are revealed by using high-velocity liquid impact as an analytical tool. The impact sites resulting from impacting the specimen with reproducible, round-fronted and coherent jets at 310 m s^{-1} from the Cavendish laboratory single-impact jet apparatus (see, for example, [7, 9, 23–25]) consist of short circumferential cracks when a well-finished zinc sulphide specimen is impacted. However, impact sites on samples from the above experiments contain long linear cracks superimposed on the typical short circumferential cracks (Fig. 5). These cracks are indicative of large flaws in the material surface. It is these flaws, probably left in the material from the grinding and polishing process, that cause the large variation in fracture stress.

It is important to discover whether the fracture stress derived for this material is dependent on the size of the sample used for the experiments. It is often easier to obtain a good surface finish on a small

specimen than on a large one. It was therefore decided that full-scale components should also be assessed using this technique and to this end seven 125 mm diameter, 5.45 mm thick, diamond-fly cut zinc sulphide discs were broken in a scaled-up version of the apparatus. A typical fracture pattern can be seen in Fig. 6. The results are included in Fig. 4 and agree within the experimental error, and encouragingly at the high end of the range, with those for the small diamond-fly cut zinc sulphide discs (batch 5), 82 $\pm$ 15 MPa compared to 99 $\pm$ 20 MPa.

3.2. Stress corrosion in zinc sulphide

The stress intensity factor versus velocity (K_I–V) graph for zinc sulphide from data from two different samples is given in Fig. 7; the relative humidity was 52%. The plateau in the graph occurs because at this point the crack is opening with sufficient velocity to prevent the corroding medium reaching the crack tip; for further discussion, see [1–5]. Fig. 8 shows the results from Fig. 7, superimposed on those for soda–lime glass and demonstrates zinc sulphide's superior resistance to stress corrosion. For comparison, the range of critical stress intensity factors previously measured is quoted in Savage [26] as 0.67–1 MPa $m^{1/2}$; the large spread is due to the data being obtained by several techniques and from different grain-size materials. The average grain size of the material used in the current study was 4 μm.

The experiments were repeated for zinc sulphide plates immersed in water. This allows the corroding medium continual access to the crack tip and should therefore remove the plateau in the results. Fig. 9 shows data from two different samples tested under these conditions. The plateau was removed as expected.

Constant load tests were attempted on the specimen at stress intensity factors at and below 0.7 MPa $m^{1/2}$ but no crack growth was observed. It is possible that

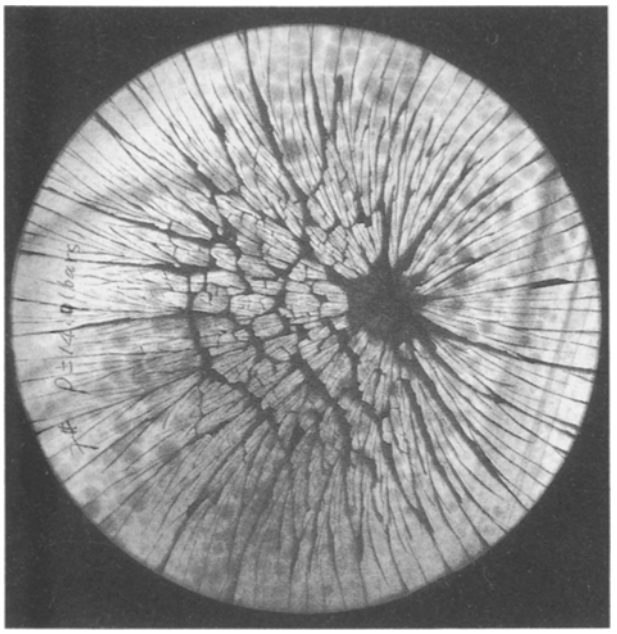

Figure 6 A typical failure pattern observed in a 125 mm diameter disc broken in the bursting disc apparatus.

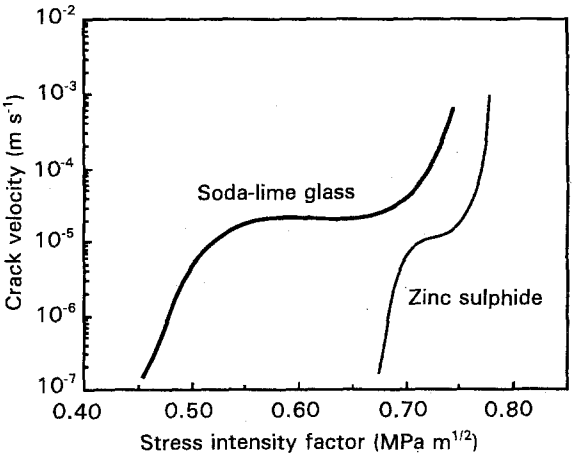

Figure 8 The variation of crack velocity with stress intensity factor for zinc sulphide and soda–lime glass in air.

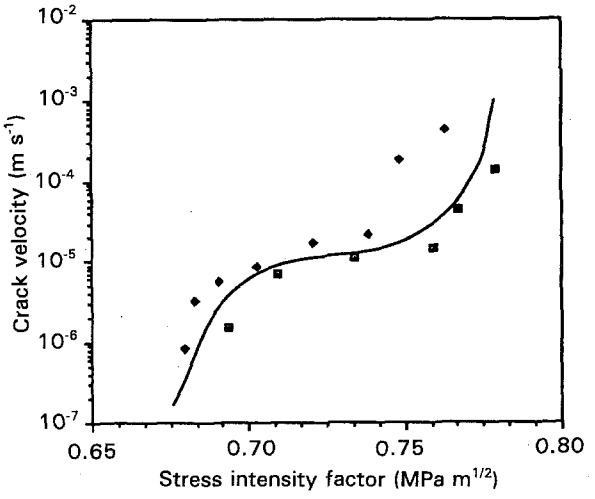

Figure 7 The variation of crack velocity with stress intensity factor for zinc sulphide in air.

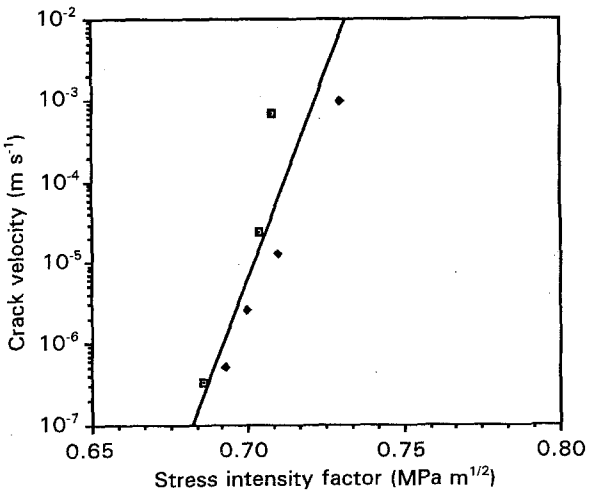

Figure 9 The variation of crack velocity with stress intensity factor for zinc sulphide in water.

this is due to crack pinning at grain boundaries. A similar microstructural interaction was observed by Quinn [16] in several materials.

3.3. The fracture stress of zinc sulphide at high and low temperatures

3.3.1. Data from the present study

The variation in fracture stress of zinc sulphide with temperature can be seen in Fig. 10 which shows the average of ten samples at each temperature and the standard deviation of the mean of the results. The samples failed in the triple cleft pattern observed by Rudnick *et al.* [21] and shown in Fig. 3 which is indicative of the required tensile failure at the disc centre. At 600 °C there was evidence of microcracking near to the anvils.

It must be emphasized at this point that because of the limitations of the Brazilian test geometry, the absolute fracture stress in Fig. 10 is not a true representation of that of the material, but the variations in strength with temperature observed in the graph are real phenomena. The average room temperature value of 52.7 MPa is approximately 75% of the baseline strength of 67 MPa obtained in Section 3.1. Allowing for the large spread in data in the experiment, this is in reasonable agreement with the result (65%) found by Hand [22] using the same geometry.

The strength of the material reaches peaks at 100 and at 300 °C and then increases up to 600 °C. Infrared spectra of samples heated to 400 °C and then cooled back to room temperature, matched those of unheated samples, suggesting that there was no permanent chemical change with temperature. It was hypothesized that the increase in strength is due to the removal of water from the surface of the specimen and the consequent reduction in the water available at the crack tip. The effect of stress corrosion is therefore reduced and the flaws in the material will not propagate until the critical stress intensity factor is reached. The fracture stress close to room temperature can be elevated by heating the specimens up to 300 °C and then allowing them to cool under vacuum over a period of about 4 h, thus further reducing the water concentration at the crack tip. In addition, the room-temperature fracture stress can be reduced by immersing the specimens in water during the test. Both of these experiments are included in Fig. 10 and support the stress corrosion hypothesis.

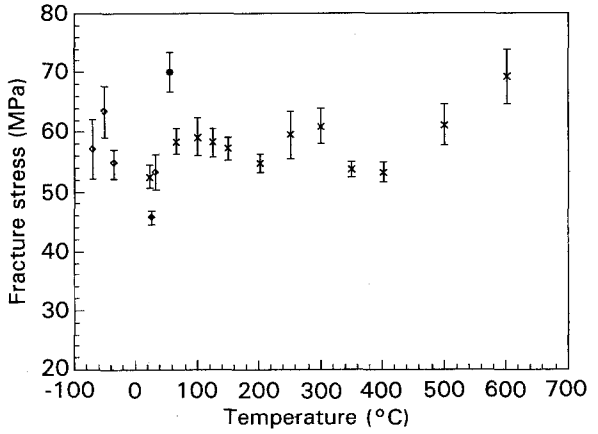

Figure 10 Zinc sulphide fracture stress data from the Brazilian test. Note that the absolute values of fracture stress are lower than those obtained by other techniques. The true values should be obtained from Fig. 4. (×) High-temperature batch, (◇) low-temperature batch, (◆) immersed in water, (●) heated to 300 °C then cooled to 55 °C.

The samples provided for the low-temperature experiments were from a different batch of zinc sulphide than those used above, and appeared noticeably paler although the preparation processes were nominally the same in the two cases. The room-temperature results were therefore repeated for the second batch and compared with those for the first batch. The two values are identical to within 2%. The low-temperature results, taken at − 35, − 50 and − 70 °C showed a slight increase in strength, which could again be explained by a reduction in the effects of stress corrosion.

3.3.2. Analysis

Both Schwartz [27] and Deom *et al.* [28] predict a steady increase in zinc sulphide fracture strength with temperature. These experiments were conducted in air rather than the nitrogen atmosphere of the present study and the increase observed in the literature data we suggest is due to crack-tip blunting by oxidation [29, 30] and by the reduction in the amount of adsorbed water. Earlier results by Hand [22] using the same Brazilian test rig in a nitrogen environment and a limited number of samples agree well with the present data and included evidence of both plasticity and a decrease in strength at 700 °C. This fracture stress reduction with plasticity is characteristic of high-temperature strength data on ceramics [30, 31].

The mechanisms for the slight variations in strength in Fig. 10 are more difficult to discern. Xue and Raj [32] presented results that suggest that intergranular cavitation and grain growth are minimal at temperatures below 950 °C for zinc sulphide. Crack blunting through dissolution in, and reprecipitation from, atmospheric and adsorbed water has been discussed at length for glass [33–35]. There seems, however, to be very little reaction between zinc sulphide and water at these low temperatures [36, 37]. For these reasons the variations in strength are most likely to be due to the effects of stress corrosion varying with temperature and the amount of adsorbed water below 300 °C and the onset of plasticity and microcracking at the higher temperatures.

4. Conclusion

The room-temperature strength evaluation showed that the samples tested had a low average and a large spread in fracture stress. Impact with a high-velocity liquid jet revealed that this was in part due to large flaws left in the specimen from the grinding and polishing process. The full-size diamond-fly cut components gave similar fracture stress values to those of the 25 mm test coupons suggesting that both the

specimen preparation procedure and the bursting disc test itself are independent of the specimen size.

The double-torsion geometry is a useful technique which produces very valuable data but only if the test is designed and performed with great care. The experiments on zinc sulphide showed that it is susceptible to stress corrosion but to a lesser extent than soda–lime glass.

The most important result from the high- and low-temperature strength data is that in the nitrogen atmosphere the average fracture stress in the range -70 to $+600\,^{\circ}C$ is equal to or greater than the room-temperature value. The infrared window can therefore be designed using the room-temperature fracture stress of zinc sulphide. The variations in strength observed are most likely to be due to the effects of stress corrosion.

Acknowledgements

The authors thank Jin Ying Liu and K. Fagan for technical support and Dr J. A. Savage, DRA, Malvern, and D. Chamberlain (ex BAe) for advice and providing samples. This work has been carried out with the support of the Defense Research Agency (Malvern).

References

1. S. M. WIEDERHORN, *J. Am. Ceram. Soc.* **59** (1967) 407.
2. S. M. WIEDERHORN, A. G. EVANS, E. R. FULLER and H. JOHNSON, *ibid.* **57** (1974) 319.
3. A. G. EVANS, *J. Mater. Sci.* **7** (1972) 1137.
4. J. B. WACHTMAN, *J. Am. Ceram. Soc.* **57** (1974) 509.
5. T. A. MICHALSKE and B. C. BUNKER, *Sci. Am.* December (1987) 78.
6. S. VAN DER ZWAAG, J. T. HAGAN and J. E. FIELD, *J. Mater. Sci.* **15** (1980) 2965.
7. S. VAN DER ZWAAG and J. E. FIELD, *ibid.* **17** (1982) 2625.
8. D. TOWNSEND and J. E. FIELD, *ibid.* **25** (1990) 1347.
9. S. VAN DER ZWAAG and J. E. FIELD, *Eng. Fract. Mech.* **17** (1983) 367.
10. C. R. SEWARD, C. S. J. PICKLES, R. MARRAH and J. E. FIELD, in "SPIE proceedings 1760", San Diego, July 1992 edited by P. Klocek (International Society for Optical Engineering, P.O. Box 10, Bellington, Washington, USA).
11. M. J. MATTHEWSON and J. E. FIELD, *J. Phys. E* **13** (1980) 355.
12. E. R. FULLER Jr, in "Fracture mechanics Applied to Brittle Materials" ASTM STP 678 edited by S. W. Freiman (American Society for Testing and Materials, Philadelphia, PA, 1979) p. 3.
13. B. J. PLETKA, E. R. FULLER Jr and B. G. KOEPKE, *ibid.*, p. 19.
14. R. B. TAIT. P. R. FRY and G. G. GARRETT, *Exp. Mech.* March (1987) 14.
15. T. A. MICHALSKE, M. SINGH and V. D. FRECHETTE, "Fracture Mechanics Methods for Ceramics, Rocks and Concrete", ASTM STP 745 (American Society for Testing and Materials, Philadelphia, PA, 1981) p. 3.
16. G. D. QUINN, *J. Mater. Sci.* **22** (1987) 2309.
17. F. L. L. E. CARNEIRO and A. BARCELLOS, *Bull. RILEM* **13** (1953) 97.
18. G. HONDROS, *Aust. J. Appl. Sci.* **10** (1959) 243.
19. H. AWAJI and S. SATO, *J. Eng. Mater. Tech.* **101** April (1979) 1347.
20. B. W. DARVELL, *J. Mater. Sci.* **25** (1990) 757.
21. A. RUDNICK, A. R. HUNTER and F. C. HOLDEN, *Mater. Res. Stand.* **3** April (1963) 283.
22. R. J. HAND, PhD thesis, University of Cambridge (1987).
23. F. P. BOWDEN and J. H. BRUNTON, *Proc. Roy. Soc. Lond.* **A263** (1961) 433.
24. F. P. BOWDEN and J. E. FIELD, *ibid.* **A282** (1964) 331.
25. C. R. SEWARD, C. S. J. PICKLES and J. E. FIELD, in "SPIE proceedings 1326", San Diego, July 1990, edited by P. Klocek (International Society for Optical Engineering, P.O. Box 10, Bellington, Washington, USA) p. 280.
26. J. A. SAVAGE, "Infrared Optical Materials and their Antireflection Coatings" (Adam Hilger, Bristol, 1985).
27. R. W. SCHWARTZ, in "Third Workshop on Passive Infrared Optical Materials and Coatings," Brussels, Paper 4, NATO Brussels, Belgium March 1990, edited by J. A. Savage, unpublished.
28. A. A. DEOM, D. L. BALAGEAS, F. G. LATURELLE, G. D. GARDETTE and G. J. FREYDEFONT, in "SPIE proceedings 1326", San Diego, July 1990, edited by P. Klocek (International Society for Optical Engineering, P.O. Box 10, Bellington, Washington, USA) p. 301.
29. G. M. PRABHU, D. L. ULRICHSON and A. H. PULSIFER, *Ind. Eng. Chem. Fundam.* **23** (1984) 271.
30. R. W. DAVIDGE, "Mechanical Behaviour of Ceramics" (Cambridge University Press, 1979).
31. N. SHINKAI, R. C. BRADT and G. E. RINDONE, *J. Am. Ceram. Soc.* **64** (1981) 426.
32. L. A. XUE and R. RAJ, *ibid.* **72** (1989) 1792.
33. K. IKEDA, H. IGAKI, Y. TANIGAWA and K. TAGASHIRA, *ibid.* **73** (1990) 2114.
34. W. HAN and M. TOMOZAWA, *ibid.* **72** (1989) 1837.
35. K. HIRAO and M. TOMOZAWA, *ibid.* **70** (1987) 43.
36. D. BRION, *Appl. Surf. Sci.* **5** (1980) 133.
37. H. Y. SOHN and K. DAESOO, *Metall. Trans. B* **18** (2) (1987) 451.

Received 26 July
and accepted 9 September 1993